Journal of Alloys and Compounds 721 (2017) 392–404

Contents lists available at ScienceDirect

Journal of Alloys and Compounds

journal homepage: http://www.elsevier.com/locate/jalcom

Enhancement of discharge properties of an extruded Mg-Al-Pb anode for seawater-activated battery by lanthanum addition

Yinchun Shi, Chaoqun Peng, Yan Feng*, Richu Wang, Naiguang Wang

School of Materials Science and Engineering, Central South University, Changsha, 410083, China

A R T I C L E I N F O

Article history:
Received 16 November 2016
Received in revised form
19 April 2017
Accepted 26 May 2017
Available online 26 May 2017

Keywords:
Mg-Al-Pb alloy
Lanthanum
TEM
Grain orientation
Corrosion behavior
Discharge performance

A B S T R A C T

Mg-Al-Pb alloys are a typical anode material for seawater-activated batteries. The microstructure and electrochemical corrosion behavior of a Mg-Al-Pb alloy fabricated by extrusion, with and without lanthanum, were investigated in this study. The results indicated that the addition of lanthanum led to the formation of β-$Al_{11}La_3$ and promoted recrystallization. The extruded Mg-Al-Pb-La exhibited less dislocations and twin defects than the extruded Mg-Al-Pb, contributing to its improved corrosion resistance. A single battery with a Mg-Al-Pb-La anode and CuCl cathode exhibited a higher cell voltage than that using a Mg-Al-Pb anode. The power density of the former was 260.8 mW cm^{-2} discharged at 300 mA cm^{-2}, which were higher values than those of Mg-H_2O_2 semi-fuel batteries.

1. Introduction

Seawater-activated batteries are receiving increasing attention due to their superior practicability and low cost compared to conventional alkaline and lithium batteries, leading to the broad application of this battery in many submarine devices [1]. It is of great scientific importance to select appropriate anode materials for seawater-activated batteries because the anode plays a vital role in maintaining the cell voltage and preventing self-discharge [2,3]. Magnesium is a good anode material owing to its high Faradic capacity of 2.2 A h g^{-1}, low density of 1.74 g cm^{-3}, and negative electrode potential of −2.37 V (vs. standard hydrogen electrode (SHE)) [3–7]. Mg-Al-Pb alloys are typical anode materials for such battery applications because of their strong discharge activity [2,3]. However, magnesium has poor corrosion resistance, and various methods for enhancing the electrochemical corrosion performance of magnesium have been investigated, including alloying, plastic deformation, and heat treatment [1–3,7–11].

Firstly, alloying elements, especially rare earths (REs), have been extensively used to enhance the electrochemical corrosion resistance of magnesium [2,10,12–15]. REs are good alloy candidates as they provide functions such as melt purification, lattice distortion, and cathode passivation [10,12,14–17]. For instance, the discharge activity and utilization efficiency of the AP65 alloy (Mg-6%Al-5%Pb (wt%)) at 180 mA cm^{-2} was significantly improved by cerium or lanthanum, which can be mainly attributed to the refined grains and the increasing amount of weak cathodic rare earth phases [18,19]. Mg-Al-Pb-Ce-Y alloy has been shown to have enhanced corrosion resistance at open circuit potential (OCP) and better discharge performance than Mg, AZ31 (Mg-3%Al-1%Zn (wt%)), and Mg-Al-Pb alloys because of the modified microstructures induced by the REs [3]. Zhang et al. [12] demonstrated that the addition of Nd to the extruded AZ91 alloy led to a reduction in crystal defects and the formation of the Al_3Nd phase, which clearly inhibited micro-galvanic corrosion, resulting in a higher corrosion resistance. A similar study by Arrabal et al. [10] that the as-cast AZ91 alloy with Nd addition exhibited a lower corrosion rate compared with unmodified AZ91 as a result of refined β phases and suppressed micro-galvanic corrosion. The corrosion resistance of the AM60 alloy was also significantly improved by the addition of both Ce and La because of its modified microstructure [20]. A critical amount of lanthanum made Mg-Hg-Ga alloy more resistant to corrosion, which was also closely associated with the refinement of grains and the formation of $Mg_{17}La_2$ and $LaHg_6$ phases acting as weak cathodes during corrosion [21]. A Mg-air battery based on Mg-Al-Pb-Ce-Y and Mg-Li-Al-Ce-Y anodes showed higher power density,

* Corresponding author. School of Materials Science and Engineering, Central South University, Changsha, Hunan, China.
E-mail address: fengyanmse@csu.edu.cn (Y. Feng).

http://dx.doi.org/10.1016/j.jallcom.2017.05.267
0925-8388/

stronger discharge activity, and higher anodic efficiency than those with pure Mg and AZ31 anodes [3,7]. In both cases, the improved performance of the Mg-air batteries was attributed to their modified microstructures after RE addition and looser discharge products.

Secondly, plastic deformation and heat treatment can also have significant effects on the electrochemical corrosion behavior of magnesium, by changing its microstructure [8,9,22,23]. Generally, plastic deformation leads to a deterioration in the corrosion resistance of magnesium because of the rearranged β ($Mg_{17}Al_{12}$) phases, deformed grains, and increased density of crystal defects, which are strongly supported by many reports [24–26]. However, Jeong et al. [23] found that the corrosion resistance of a Mg-Ca alloy with Ca ≥ 1% was enhanced by extrusion, which was closely related to the effective break-up of Mg_2Ca phases. A similar effect was reported by Minárik et al. [27] for an equal channel angular pressed (ECAPed) AZ42 alloy. It is worth noting that plastic deformation often gives rise to variations in the grain orientation, which in turn has an obvious effect on the electrochemical corrosion behavior of magnesium [8,28,29]. Normally, the basal crystal plane (0001) exhibits lower surface energy and is much more corrosion resistant than the non-basal ones [28,29]. The rolling surfaces of rolled AP65 and AZ31 alloys have a much higher proportion of basal crystal planes, and thus, they usually exhibit lower corrosion rates than a cross-sectional surface, owing to the lower surface energy of the basal planes [8,28]. Heat treatment has an obvious effect on the evolution of secondary phases and thus promotes or suppresses micro-galvanic corrosion between secondary phases and the matrix; the latter improving the electrochemical corrosion properties of magnesium alloys [9]. For instance, rolled and subsequently annealed AP65 alloy exhibited a good discharge performance when discharged at 180 mA cm^{-2} due to the refined grains, uniform grain size, and good compositional homogeneity [8]. The large number of dispersed $Mg_{21}Ga_5Hg_3$ phases precipitated during the aging process significantly promoted the self-catalyzed reaction of the Mg-8.8Hg-8Ga (wt%) alloy, which was in favor of the activation dissolution of the matrix and the improved discharge performance [9].

In this work, lanthanum was chosen as the alloying element for a Mg-Al-Pb alloy. The effect of lanthanum on the corrosion behavior at open circuit potential (OCP) and the performance during discharge were systematically studied considering the formation of secondary phases, crystal defects, and grain orientation.

2. Experimental methods

2.1. Materials preparation

The nominal compositions (wt%) of the Mg-Al-Pb (referred to as AP65) and Mg-Al-Pb-La (referred to as AP65-La) alloys were Mg-6% Al-5% Pb-0.5% Zn-0.1% Mn and Mg-6% Al-5% Pb-0.5% Zn-0.1% Mn-1% La, respectively. These alloys were prepared using melting and casting with an induction furnace under argon atmosphere at 750 °C. Mn and La were added via Al-15% Mn and Mg-30% La (wt%) alloys, respectively. The other alloying elements (Al, Pb, and Zn) were added in the form of pure metals (99.99 wt%). The molten metal was then poured into a preheated iron mould. Progressive solution treatments at 330 °C for 16 h and then 420 °C for 2 h were performed on the as-cast alloys, followed by water quenching. The as-quenched ingots were preheated at 450 °C for 18 h, and then extruded into rods with a diameter of 40 mm at an extrusion speed of 3 m min^{-1} and an extrusion ratio of 9:1. The chemical compositions of the two alloys were analyzed using inductively coupled plasma atomic emission spectrometry (ICP-AES). The results showed that the impurity concentrations were less than 0.1 wt% and the deviation from the intended stoichiometry for all elements was lower than ±2.0%.

2.2. Microstructure characterization

The microstructures of the extruded AP65 andAP65-La alloys were observed using optical microscopy (OM; XJP-6A metallurgical microscope) and scanning electron microscopy (SEM; FEI-Quanta 200). The compositions of phases were detected using electron probe micro-analysis (EPMA; JXA-8230). In addition, transmission electron microscopy (TEM; Tecnai G2 F20) and electron backscatter diffraction (EBSD; Helios Nanolab 600i) were employed to further investigate the crystal defects and grain orientations, respectively. Transverse sections along the radial direction (RD) and longitudinal sections along the extrusion direction (ED) are depicted in Fig. 1.

The specimens used for metallographic observation were ground several times with increasingly fine grades of SiC abrasive papers and polished with diamond grinding paste (0.5 μm). These samples were then etched with a solution of 2.5 mL of acetic acid, 5 mL of distilled water, 50 mL of ethanol, and 3 g of picric acid to reveal the grain boundaries. The linear intercept method was used to evaluate the grain sizes of the extruded AP65 and AP65-La alloys from OM images using Nano Measurer 1.2 software. The number of grains considered in this analysis was 200 for each alloy. An electron discharge cutter was used to cut thin samples for TEM and EBSD observation, which were then ground to a thickness of 70 μm using abrasive papers. Lastly, the thin foils were ion milled with an ion beam thinner (Gatan 691). The specimens used for corrosion morphology observations were immersed in an aqueous solution of 3.5 wt% NaCl for 1 min and 72 h, respectively. Thereafter, the corrosion products were cleaned using chromic acid (200 g L^{-1} CrO_3 +10 g L^{-1} $AgNO_3$) in an ultrasonic bath. The 3.5 wt% NaCl solution was made with analytical grade chemicals and distilled water to simulate seawater [1,8–10].

2.3. Weight loss measurements

The weight loss measurements were conducted to investigate the corrosion resistance at OCP. The specimens used for weight loss measurements were ground with SiC abrasive papers and weighed using a digital balance with a precision of 0.1 mg to obtain the original weight. Then they were immersed in 3.5 wt% NaCl aqueous solution at 25 °C for 72 h and cleaned in the same chromate solution described above and then absolute ethyl alcohol. Finally, the specimens were dried in a flow of hot air and weighed again to quantify the weight loss rate. In addition, the weight loss rate (ΔW, mg cm^{-2} d^{-1}) can be converted into the average corrosion rate (P_w, mm y^{-1}) via $P_w = 2.10 \cdot \Delta W$ [30].

2.4. Electrochemical measurements

The corrosion behavior at OCP and the discharge performance of

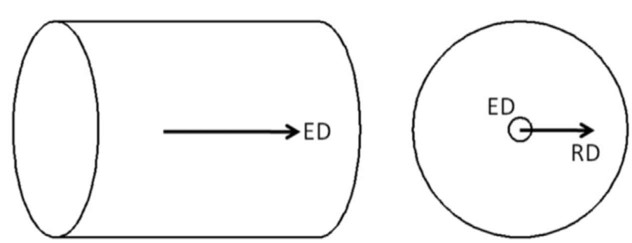

Fig. 1. Sampling directions in the extruded AP65 and AP65-La alloys (Longitudinal sections along the extrusion direction (ED) and transverse sections along the radial direction (RD)).